

PACS numbers: 42.55.Mv; 42.60.Lh
DOI: 10.1070/QE2014v044n03ABEH015252

Lasing characteristics of difluoroborates of 2,2′-dipyrromethene derivatives in solid matrices

R.T. Kuznetsova, Yu.V. Aksenova, T.A. Solodova, T.N. Kopylova, E.N. Tel'minov, G.V. Mayer, M.B. Berezin, E.V. Antina, S.L. Burkova, A.S. Semeikin

Abstract. **The luminescence-spectral, lasing and photochemical characteristics of laser media based on boron fluoride complexes of dipyrromethenes, embedded into solid bulk matrices of polymethylmethacrylate and its modifications (obtained by adding polyhedral oligomeric silsesquioxane during polymerisation) and into polymer films, in which polyhedral silsesquioxane enters the composition of monomeric unit, have been investigated.**

Keywords: *dipyrromethene derivatives, coloured solid matrices and films, lasing spectra, polyhedral silsesquioxane nanoparticles, resource characteristics.*

1. Introduction

Tunable lasers based on organic molecules, which have broadband gain and stimulated emission spectra, can be used in high-technology optical production, for example, as sources of coherent tunable excitation radiation in spectroscopic instrument engineering and in separation of isotopes. Note that, despite the development of alternative sources, these lasers remain very popular [1–12]. Solutions of organic compounds as lasing media have been studied for a rather long time. However, application of solid polymer matrices or films doped with complex organic luminophors instead of solutions is most attractive from the practical point of view and for miniaturisation of these devices. These factors stimulate studies of the properties of solid samples [5, 8, 9, 11–14]. Note that rather stringent requirements to both the conversion efficiency of pump radiation and the photostability under high-power optical excitation are imposed on organic dyes-luminophors, because specifically photoconversion processes are responsible for the resource characteristics of these devices [6–10]. Studies of different research teams showed that the efficiency and, especially, photostability of coumarin, rhodamine, and polymethine laser dyes, which are used to form laser media in the entire visible spectral range, are worse than those of commercial dipyrromethene complexes (PM547, PM567, etc.) [1–7, 10, 15].

R.T. Kuznetsova, Yu.V. Aksenova, T.A. Solodova, T.N. Kopylova, E.N. Tel'minov, G.V. Mayer National Research Tomsk State University, prosp. Lenina 36, 634050 Tomsk, Russia; e-mail: kuznetrt@phys.tsu.ru;
M.B. Berezin, E.V. Antina, S.L. Burkova G.A. Krestov Institute of Solution Chemistry, Russian Academy of Sciences, ul. Akademicheskaya 1, 153045 Ivanovo, Russia;
A.S. Semeikin Ivanovo State University of Chemistry and Technology, prosp. Sheremetevskii 7, 153000 Ivanovo, Russia

Received 29 July 2013; revision received 5 December 2013
Kvantovaya Elektronika **44** (3) 206–212 (2014)
Translated by Yu.P. Sin'kov

Note that only few studies were devoted to the synthesis and analysis of fluorinated boron dipyrromethene (BODIPY) complexes with a wider circle of substituents in the core, which significantly expands the spectral range of emission [16, 17], and that there are no such studies for some substituents (for example, dibenzyl-BODIPY). An investigation of the influence of additives of polymer silsesquioxane in the form of micro- and nanoparticles to solutions and synthesised polymer matrices, which were found to ambiguously affect the lasing characteristics of dyes, has just begun [14, 18].

In this paper, we report the results of studying the luminescence spectra and laser properties [pump conversion efficiency (EFF) and resource characteristics] of BODIPY complexes of different structure, incorporated into bulk polymethylmethacrylate (PMMA) matrices and a matrix modified by adding particles of polyhedral silsesquioxane (8MMA-POSS) to methyl-methacrylate in the polymerisation stage, as well as into polymer films. The characteristics of the compounds studied were compared with their analogues in solutions for subsequent formation of compact, efficient, and photostable solid laser media.

2. Experimental

Figure 1a contains the names, structural formulas and designations of the luminophors and polymers under study. Note that the designations used here are not generally accepted; they are applied only within this paper. The compounds were synthesised, and their structure was determined by mass spectrometry, IR spectroscopy and electron spin resonance (ESR) spectroscopy at the G.A. Krestov Institute of Solution Chemistry, Russian Academy of Sciences, and the Ivanovo State University of Chemistry and Technology [19–21]. To compare the properties of solid samples and solutions as solvents, we used ethanol, ethyl acetate and cyclohexane of chemically pure grade.

The technique for synthesising solid active media based on PMMA and modified PMMA – P(MMA + 8MMA-POSS) – formed by copolymer MMA with polyhedral silsesquioxane (8MMA-POSS) (Hybrid Plastics) in amount of 13 wt% (Fig. 1b), as well as the technology for fabricating laser elements on their basis (half-cylinders 1–1.3 cm high), were described in [11, 12]. The BODIPY1 and BODIPY2 concentrations in bulk blocks were 0.5 mM.

In addition to bulk blocks, we prepared solid polymer films based on poly[(propylmethacrylheptaisobutyl-polyhedral silsesquioxane)-co-styrene] (POSS polymer), the monomeric unit of which contains polyhedral silsesquioxane in amount of 15 wt% (Sigma-Aldrich) (Fig. 1c). Films were deposited by the spin-coating method from a solution of the corresponding

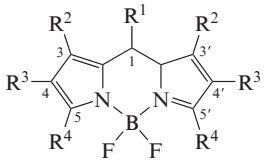

a

BODIPY1: $R^1 = H$, $R^2 = R^4 = CH_3$, $R^3 = C_2H_5$
BODIPY2: $R^1 = Ph$, $R^2 = R^4 = CH_3$, $R^3 = C_2H_5$
BODIPY3: $R^1 = H$, $R^2 = R^4 = CH_3$, $R^3 = CH_2Ph$
BODIPY4: $R^1 = R^3 = H$, $R^2 = R^4 = Ph$
BODIPY5: $R^1 = NHCH_2C^{\circ}$ CH, $R^2 = R^3 = R^4 = H$

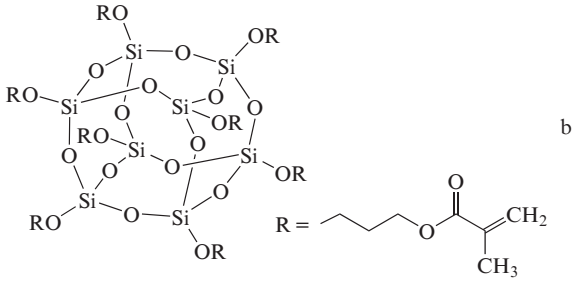

b

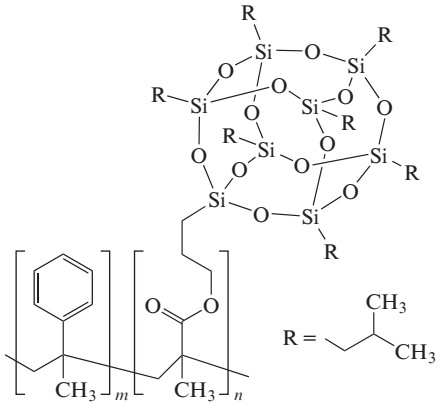

c

Figure 1. Structural formulas and designations of compounds: (a) 3,3′,5,5′-tetramethyl-4,4′-diethyl-2,2-dipyrromethene difluoroborate (BODIPY1), 3,3′,5,5′-tetramethyl-4,4′-diethyl-*meso*-phenyl-2,2′-dipyrromethene difluoroborate (BODIPY2), 3,3′,5,5′-tetramethyl-4,4′-dibenzyl-2,2′-dipyrromethene difluoroborate (BODIPY3), 3,3′,5,5′-tetraphenyl 2,2′-dipyrromethene difluoroborate (BODIPY4), and *meso*-propargylamino-2,2′-dipyrromethene difluoroborate (BODIPY5); (b) 8MMA-POSS, and (c) poly[(propylmethacrylheptaisobutyl-PSS)-co-styrene]-POSS polymer (15 wt% POSS).

BODIPY in cyclohexane (BODIPY1, BODIPY3, BODIPY4) or in ethyl acetate (BODIPY5), with addition of POSS-polymer in amount of 50 mg mL^{-1}. The dye concentration in a solution was 0.5–1 mM. The POSS polymer swelled in BODIPY solutions for 24 h under continuous stirring, and then a viscous homogeneous solution was deposited on glass substrates and centrifuged at a speed of 2000 rpm for 20–30 s. This method was used to deposit successively from 1 to 3 layers, after which the films were dried in air for 24 h. The film thickness (see Table 1) was measured using a MicroXAM-100 profilometer (USA). Note that, in contrast to bulk blocks with polished and highly uniform surfaces, through which pumping and lasing occurs, the surface of deposited films is nonuniform, especially in the case of two- and three-layer films.

The luminescence-spectral characteristics of solid elements were measured on Cary Eclipse (Varian) and SM2203 (SOLAR, Belarus) spectrometers.

BODIPY1–BODIPY4 samples were excited by the second harmonic of an LQ129 Nd:YAG laser (SOLAR) with the following characteristics: $\lambda_{las} = 532$ nm, $\tau_p = 13$ ns, $E \leqslant 70$ mJ $pulse^{-1}$, and horizontally directed electric vector (horizontal polarisation). The solutions and films coloured by BODIPY5, which does not absorb at $\lambda = 532$ nm, were pumped by the third harmonic of a LQ529B laser (SOLAR) with the parameters $\lambda_{las} = 355$ nm, $\lambda_p = 9$ ns, and $E \leqslant 30$ mJ $pulse^{-1}$ (vertical polarisation).

We used a transverse pump scheme. A cavity 2 cm long, used to implement lasing in solutions and all bulk solid elements, consisted of a highly reflecting mirror and output face of the cell or sample, i.e., the cavity parameters remained the same in all cases of pumping solutions and bulk polymer samples. Pump radiation was focused on the sample surface into a strip 0.05×0.95 cm in size. When polymer films were pumped, the cavity was absent, the excited strip was 0.06×1.4 cm in size, and radiation was generated in a planar waveguide (operating in the total internal reflection mode) and ejected out of both ends.

The power characteristics of pump and laser radiation were measured using OPHIR NOVA (Israel) and Gentec E100 (Canada) power meters with a sensitivity up to 10 μJ and an error in measuring energy of 2%. The pump intensity was varied using a set of neutral light filters. The spectral characteristics of laser radiation were measured with an AVANTES fiber laser spectrometer (the Netherlands) with an error $\Delta\lambda = 0.5$ nm.

The photoconversion quantum yield, which characterises molecular photostability, was estimated from the change in the absorption spectra of irradiated solutions after absorption of the measured amount of pump energy, as was shown in [6, 7]. The resource characteristics of bulk solid elements (lasing photostability) were determined as a number of pump pulses with a repetition rate of 2 Hz during which the laser efficiency decreased by 10% to 90% of the initial efficiency value EFF_0 (without displacement of excited volume). In addition, to perform comparison with solutions, we estimated the total pump energy P_{90}, absorbed in an excited unit volume, at which the initial lasing efficiency decreased by 10%. The absorbing (excited) volume was a right-angle prism with a height equal to the length of the pumping strip and bases in the form of triangles, penetrating the solid-element bulk. These triangles were recorded directly on the output face of the sample in the form of prints on sensitive photo paper. When measuring the resource characteristics of polymer films coloured with dyes, the absorbing volume was equal to the volume of a rectangular parallelepiped, with a base area equal to the pump spot area and a height equal to the film thickness. The absorbed pump energy was calculated taking into account the pump radiation transmitted through the thin film. An advantage of this method for estimating resource characteristics is the possibility of measuring the resource not only as a number of laser pulses during which the initial efficiency decreases to a conditional value but also in units of specific pump energy (J cm^{-3} or J mol^{-1}). This characteristic was used to compare different media and different excitation versions in [9], where samples with enhanced resource were sought for.

3. Results and discussion

3.1. Bulk polymer matrices

The spectral-fluorescent and lasing characteristics of BODIPY-coloured solid samples and (for comparison) BODIPY solu-

Table 1. Spectral-luminescence, lasing, and photochemical characteristics of BODIPY derivatives (wavelengths in nm, pump intensities in MW cm^{-2}, P_{90} in J cm^{-3}, and ε in dm^3 mol^{-1} cm^{-1}).

Compound (solvent)	λ_{abs}^{S0-S1} (ε)	λ_{fl} (λ_{ex})	$\gamma_{fl} \pm 10\%$ (λ_{ex})	λ_{las} (λ_{ex}, W_p)	EFF_{las} (%) (λ_{ex}, W_p)	$\varphi_{ph} \times 10^5$ (λ_{ex}, W_p) [P_{90}]
BODIPY1 (ethanol)	538 (57 400)	545 (475)	0.82 (475)	560 (532, 25)	74 (532, 25)	7 (532, 25) [500]
(cyclohexane)	532 (91 600)	544 (470)				
BODIPY1 PMMA matrix	528	555 (450)		558.7 (532, 3)	38 (532, 3) 70 (532, 20)	(532, 3) [720]
BODIPY 1 PMMA matrix + 8MMA-POSS	536	557 (450)		562–566 (532, 3)	58 (532, 3) 90 (532, 70)	(532, 3) [762]
BODIPY1 POSS-polymer film, l = 4 μm	535	544 (470)		560–570 (532, 15)		
BODIPY2 (ethanol)	522 (72 650)	538 (470)	0.83 (470) 0.18 (330)	551 (532, 25)	56 (532, 25)	4 (532, 20) [1800]
(cyclohexane)	526 (64 700)	543 (470)				
BODIPY2 PMMA matrix	522	551 (450)		556.4 (532, 3) 558.6 (532, 20)	32 (532, 3) 57 (532, 70)	(532, 3) [3690]
BODIPY3 (cyclohexane)	531 (119 380)	539 (500)	0.98 (500)	557 (532)	76 (532, 40)	(532, 20) [650]
BODIPY3 POSS-polymer film, l = 8 μm	534	556		569 (532, 45)	20 (532, 12)	(532, 12) [4803]
BODIPY4 (cyclohexane)	568 (28 500)	601 (550)	0.9 (520)	604 (532, 15)	7.8 (532, 40)	
BODIPY4 POSS-polymer film, l = 7 μm	570	605 (550)		605–612 (532, 40)		
BODIPY5 (ethyl acetate)	409 (37 390)	470 (370)	0.9 (370)	475 (355, 1) 478 (355, 70)	38 (355, 10)	400 (355) [7]
BODIPY5 POSS-polymer film, l = 7 μm	416	490 (370)		493 (355, 15)		

tions are listed in Table 1. These data show that the influence of substituents in BODIPY ligand is determining for the spectra of these compounds. Alkyl and benzyl substitutions in the BODIPY core provide fluorophors with maximum emission in the range of 540–570 nm (BODIPY1, BODIPY3). When a substituted amino group is introduced into the *meso*-position (R^1) or phenyl fragments over the BODIPY periphery, the spectral range of the fluorescence peak changes from 470–480 (BODIPY5) to 599–601 nm (BODIPY4) in solutions and from 490 to 605 nm in solid samples. Quantum-chemical calculations [22] showed that the presence of four phenyl cycles (BODIPY4), which barely deviate from the core plane, expands the π-system, thus causing a red shift of spectral characteristics. Since the structure close to planar is optimal and the rotation barriers of phenyl cycles are high, the fluorescence yield is also high (Table 1). Small EFF_0 values for BODIPY4 solutions are due to transient absorption in the range of lasing from excited states [22]. At the same time, the introduction of a substituted amino group into the *meso*-position (R^1) (Fig. 1a, BODIPY5) leads to a blue shift of absorption bands by approximately 90 nm and fluorescence bands by about 40 nm in comparison with the unsubstituted BODIPY. At the same time, BODIPY5 is an excellent fluorophor, which can be used as a laser-active medium for the blue-green spectral region. This compound was used for the first time as an active medium in [16]. In our study we obtained a higher lasing efficiency upon BODIPY5 excitation by the third harmonic of a Nd:YAG laser but a lower resource.

Incorporation of 8MMA-POSS into a polymer matrix containing BODIPY1 causes an additional red shift of the fluorescence peak, which indicates a decrease in the polarity of the medium in these samples (Table 1). The lasing spectra occupy the long-wavelength wing of the fluorescence spectra of both solutions and solid samples (Fig. 2). The data in Table 1 indicate that the pump conversion efficiency into laser radiation by solid samples is not lower than in solutions and is much higher for the PMMA sample coloured by BODIPY1 (with 8MMA-POSS introduced). Figure 3 shows dependences $EFF(W_p)$, which indicate that all solid samples have low lasing thresholds (less than 1 MW cm^{-2}) and do not exhibit a decrease in efficiency at high pump levels (above 50 MW cm^{-2}).

The highest efficiency (up to 90%) was obtained for the BODIPY1 sample in the modified matrix P(MMA + 8MMA-POSS): at a pump energy E = 50 mJ the output energy is 45 mJ (Fig. 3). This sample is characterised by the lowest lasing threshold (less than 0.2 MW cm^{-2}); at W_p = 0.4 MW cm^{-2} the efficiency reaches 9%. The lasing spectrum of BODIPY1 in the unmodified PMMA matrix is smooth, with a peak in the vicinity of 558 nm, whereas the spectrum of a matrix modified by introducing 8MMA POSS, under similar excitation conditions, contains several narrow peaks, each with a half-width less than 1 nm (Fig. 2a). The presence of several narrow peaks is more

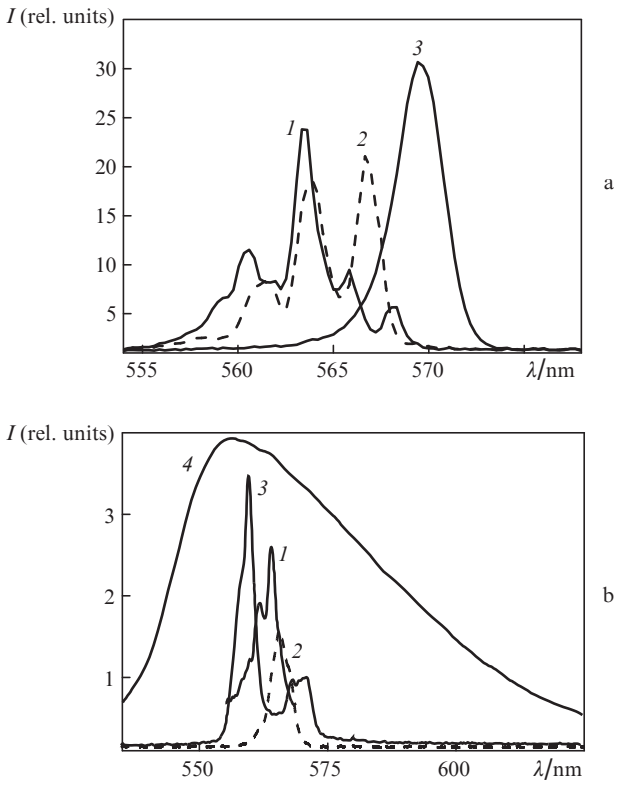

Figure 2. (a) Lasing spectra of BODIPY1 in the P(MMA + 8MMA-POSS) matrix (*1*, *2*) after excitation by the first pump pulse, recorded from different portions of generating volume, and (*3*) after a series of laser pulses, leading to a decrease in the lasing efficiency by 10% (W_p = 3 MW cm^{-2}), λ_{max} = 569.7 nm. (b) (*1*–*3*) Lasing spectra of BODIPY1 in (*1*, *2*) P(MMA + 8MMA-POSS) matrix and (*3*) POSS-polymer film and (*4*) a fluorescence spectrum of BODIPY1 in P(MMA + 8MMA-POSS) matrix: (*1*, *3*) after excitation by the first pump pulse and (*2*) after generation of a series of pulses (W_p = 20 MW cm^{-2}, λ_{max} = 565.5 nm).

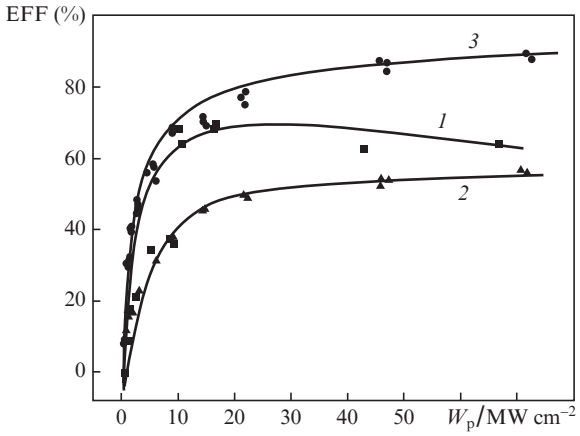

Figure 3. Dependences of the conversion efficiency of the second harmonic of Nd:YAG laser into laser radiation on its intensity for (*1*, *2*) solid samples based on PMMA and (*3*) samples with incorporated 8MMA-POSS (13 wt%). The samples are coloured by (*1*, *3*) BODIPY1 and (*2*) BODIPY2.

pronounced at low excitation intensities (W_p = 3–8 MW cm^{-2}). With an increase in the pump intensity, the peaks broaden and merge, thus reducing their total number in the spectrum [Fig. 2b, curve (*1*)]. On the whole, the centroid of the BODIPY1 lasing spectrum in the modified P(MMA + 8MMA-POSS) sample is located in the longer wavelength region (λ_{max} = 564 nm) in comparison with the same PMMA sample (λ_{max} = 558 nm) (Fig. 2, Table 1).

A comparison of the energy and spectral lasing parameters of BODIPY1 and BODIPY2 in a bulk PMMA matrix shows qualitative correspondence between the lasing characteristics and the similar characteristics for solutions in ethanol (Table 1). The lasing efficiency of solid samples under identical pump intensities for BODIPY1 is higher than for BODIPY2, and the emission spectra of BODIPY1 in a PMMA matrix are in the longer wavelength range (as compared with the BODIPY2 spectra); this tendency is also observed for the solutions of these compounds. With an increase in the pump intensity, the lasing spectra of the solid samples coloured by BODIPY1 and BODIPY2 are red-shifted by 3–4 nm (as in solutions) [6, 7]. A comparison of the BODIPY1 characteristics in the conventional PMMA matrix and in the modified matrix reveals the influence of 8MMA-POSS particles on the lasing characteristics of samples (increase in efficiency and reduction of threshold). On the one hand, these features of lasing spectra can be related to bulk inhomogeneities and different degrees of quality of the end face treatment (nonparallelity, sphericity, axis misalignment), which may manifest itself in the multispike structure of spectrum. At the same time, our results are in agreement with the data of [14, 18] for a number of dyes in solutions and bulk polymer matrices, which are also indicative of enhanced efficiency and reduced threshold under generation of laser-like radiation in samples containing 8MMA-POSS nanoparticles (13%) in comparison with unmodified samples.

It was also reported in [18] that the thermal conductivity in a modified PMMA matrix increases from 0.182 W m^{-1} K^{-1} for a pure matrix to 0.233 W m^{-1} K^{-1} for a matrix containing 50% 8MMA-POSS, which may affect the improvement of laser characteristics. However, this is not the main source of the aforementioned features, because a similar increase in silicon-containing gel matrices does not lead to improvement of laser characteristics [23]. The lasing features indicated above were explained in [14, 18] by the increase in the photon mean free path in the cavity because of the scattering of radiation from nanoparticles; specifically this factor causes a decrease in the lasing threshold and an increase in the lasing efficiency.

3.2. Films based on POSS polymer

The data of Table 1 indicate that the fluorescence and lasing spectra of solid POSS-polymer films coloured by different BODIPY dyes are red-shifted (as well as those of bulk matrices) with respect to the similar spectra of solutions. Since the films are thin, the POSS-polymer film coloured by BODIPY3 is most favourable for measuring efficiency in comparison with other compounds, because in this case pumping is performed practically to the peak of the long-wavelength absorption band. The efficiency for this film, with allowance for the pump transmission and two-sided ejection of generated radiation in a planar waveguide, is 20% at W_p = 15 MW cm^{-2}; it decreases to 14% at W_p = 60 MW cm^{-2}. For other BODIPY dyes, the absorbed energy is much lower; therefore, the lasing energy is below the OPHIR sensitivity threshold and the efficiency cannot be determined. The films based on POSS polymer also have spectra with several peaks (Fig. 2b). Cerdan et al. [14] reported red shifts and multispike structure of lasing spectra in PMMA films of alkyl-substituted pyrromethene 567 (PM567) with addition of 8MMA-POSS; these features arise only when the concentration of the latter component is no less than 50%.

They were explained in [14, 18] by the scattering of amplified radiation from POSS nanoparticles. An additional study must be performed to gain a deeper insight into the nature of the specific features of lasing in a PMMA matrix modified by 8MMA-POSS.

The spectral characteristics of lasing in POSS-polymer solutions, matrices, and films coloured by BODIPY derivatives (see Table 1) indicate that the lasing range of the BODIPY complexes under study begins with the blue-green region (470–510 nm) and covers the yellow-orange (550–580 nm) and red (580–620 nm) regions, which is very important for practical application of these media (provided that they have a sufficient resource).

3.3. Resource characteristics of solid samples

The resource characteristics for a number of BODIPY alkyl derivatives as laser media (PM567, PM597) were reported in [4–9, 18, 24]; however, as was noted above, their direct comparison can hardly be performed.

First, it should be noted that both the molecular and lasing photostability in a solution is very low for the efficient active medium based on BODIPY5, which generates in the blue-green spectral region with $EFF_0 = 38\%$: the photoconversion quantum yield in ethyl-acetate is two orders of magnitude higher than, for example, for an ethanol solution of BODIPY2. However, one should take into account that BODIPY5 was studied upon UV excitation with $\lambda_p = 355$ nm, whereas BODIPY2 was excited by radiation with $\lambda_p = 532$ nm (Table 1). The resource of the BODIPY5-based laser medium, which generates in a very important spectral region, is of great importance; thus, further study of its photostability must be performed with a purpose of increasing the resource by changing the excitation wavelength and improving the molecular photostability (the latter currently does not exceed the photostability of coumarin dyes, which generate in the same blue-green region).

Figure 4 shows the relative lasing efficiencies of solid bulk PMMA matrices with BODIPY1 and BODIPY2 as functions of the number of lasing pulses and of the total absorbed pump energy per irradiated unit volume at an excitation intensity $W_p = 3$ MW cm^{-2}. One cannot see that, under these conditions, the sample coloured by BODIPY2 has the longest service life: $P_{90} = 3690$ J cm^{-3} (10 600 pulses).The samples coloured by BODIPY1, both in pure PMMA and in modified P(MMA + 8MMA-POSS) compound, have a much smaller resource than BODIPY2 in the PMMA matrix; they differ only slightly ($P_{90} = 720$ and 762 J cm^{-3}, respectively) and exceed greatly the resource for ethanol solution of BODIPY1 (Table 1). The numbers of pulses corresponding to this decrease in the initial value EFF_0 are, respectively, 4500 and 2400. This inconsistency of resource characteristics in different units of measurement (J cm^{-3} and number of pulses) is due to the difference in the emitting volumes absorbing pump radiation in solid samples. In the case of modified P(MMA + 8MMA-POSS) matrix, the absorbing (generating) volume is smaller than that in the pure PMMA matrix by almost half. Since both matrices have identical BODIPY1 concentrations, we can suggest in this stage that the decrease in the excited volume, i.e., the decrease in the penetration depth of pump radiation in the matrix with incorporated 8MMA-POSS is due to the multiple scattering of pump radiation from POSS nanoparticles. This question also calls for further study.

The results obtained for samples of BODIPY1 and BODIPY2 in a pure PMMA matrix are in qualitative agreement with the

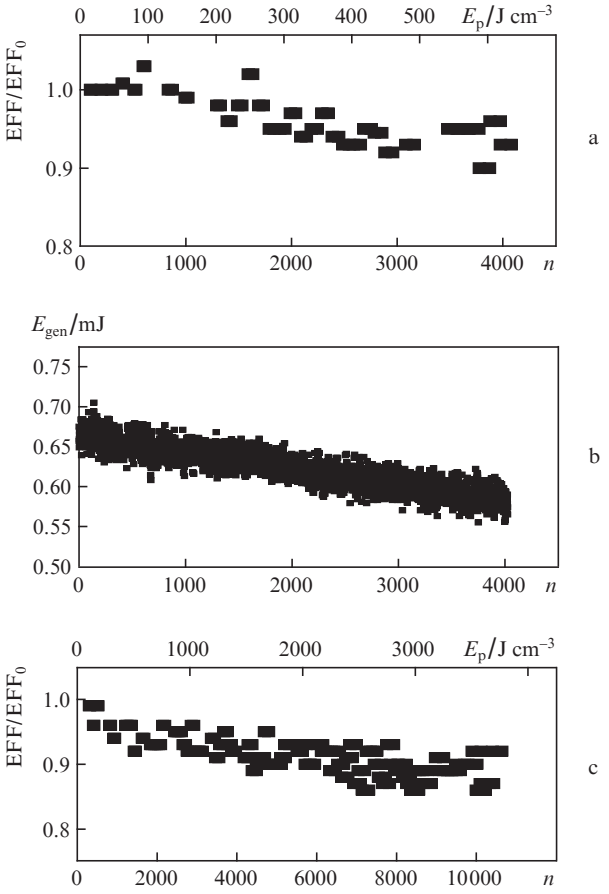

Figure 4. Dependences of the (a, c) relative lasing efficiency on the number of pulses n and the total pump energy absorbed in unit volume and the (b) dependence of the lasing pulse energy E_{gen} on the number of pulses for (a, b) BODIPY1 and (c) BODIPY2 samples in a solid PMMA matrix. P_{90} = (a, b) 720 J cm^{-3} (4500 pulses) and (c) 3690 J cm^{-3} (10 600 pulses); $W_p = 3$ MW cm^{-2}; and EFF_0 = (a, b) 38% and (c) 32%.

photostability characteristics of these compounds in solution (Table 1). This means that the decrease in the efficiency during lasing in both solutions and solid matrices is due to photoconversions, which are approximately twice as efficient for BODIPY1 in solution than for BODIPY2 (under the same conditions of excitation by the second harmonic of Nd:YAG laser) (Table 1).

The increase in the lasing photostability in solid samples in comparison with the photostability in solutions (Table 1) is in agreement with the results obtained by us for other laser dyes [24] and for BODIPY derivatives [9]. This phenomenon is explained by partial geminal recombination of intermediate photoproducts in the solid matrix, whereas the recombination of photoproducts formed in solutions is hindered by the mobility of the solvate shell.

The results presented in Fig. 4 were obtained for a low excitation intensity, i.e., for non-optimal initial efficiency (Fig. 3). An attempt to increase EFF_0 of BODIPY-containing solid samples by increasing the pump intensity was no success. Beginning with an intensity of 9 MW cm^{-2}, cracks began to form in the generation region of the samples with BODIPY1 in P(MMA + 8MMA-POSS) and BODIPY2 in PMMA after a large number of excitation pulses. This process led to a significant drop of efficiency, which was not caused by dye photoconversions but was only due to the damage of the solid matrix during stimulated emission. Cracks arose not on the

Table 2. Lasing intensities W_{las} for bulk matrices coloured by BODIPY at different excitation intensities.

W_p/ MW cm^{-2}	W_{las} / MW cm^{-2} BODIPY1, PMMA matrix	W_{las} / MW cm^{-2} BODIPY1, PMMA + 8MMA-POSS matrix	W_{las} / MW cm^{-2} BODIPY2, PMMA matrix
3	15.5	40	28
9		132	
15	51	365	200
23			264

sample surface (up to the intensity W_p = 70 MW cm^{-2}) but in the generation volume. The data of Table 2 showed that, for the sample of BODIPY1 in P(MMA+ 8MMA-POSS), which is characterised by the highest lasing efficiency, the lasing intensity W_{las} at W_p = 15 MW cm^{-2} and EFF$_0$ = 69% is on average 365 MW cm^{-2} (at this intensity the matrix undergoes fracture). This value decreases to 132 MW cm^{-2} at W_p = 9 MW cm^{-2}. However, microcracks arise even under these conditions. In the unmodified PMMA matrix, coloured by BODIPY1, the lasing intensity decreases both due to the lower efficiency and due to the enlarged excitation volume. Even at a pump intensity of 15 MW cm^{-2} the laser intensity does not exceed 50 MW cm^{-2} (Table 2). Hence, microcracks are absent under these conditions, and the resource, measured for this sample at W_p = 15 MW cm^{-2} (P_{90} = 750 J cm^{-3}), is close to the corresponding resource measured at W_p = 3 MW cm^{-2}.

The PMMA sample, coloured by BODIPY2, is characterised by a small generation volume; therefore, its service life can also be long only at $W_p \leqslant 3$ MW cm^{-2}.

As was noted above, concerning POSS-polymer films of micrometer thicknesses, quantitative resource characteristics can be obtained for only films coloured by BODIPY3. Since the generation volume in a 8-μm-thick film is small, the decrease in EFF$_0$ from 20% to 18% at an intensity W_p = 12 MW cm^{-2} occurs after 204 pulses, which corresponds (with allowance for the transmission T = 77%) to P_{90} = 4803 J cm^{-3}. This value is close to the resource of the solid bulk matrix coloured by BODIPY2. The lasing intensity for this film is 78 MW cm^{-2}; however, the film does not loose integrity under these conditions, which can be related to the small number of pump pulses absorbed within this volume.

When studying the resource characteristics, the lasing spectra were recorded both before and after measuring the resource in the same volume of solid samples. The spectrum of the solid sample of BODIPY1 in the modified P(MMA + 8MMA-POSS) matrix irradiated at W_p = 3 MW cm^{-2} lacked a multispike structure and exhibited a more pronounced red shift of the centroid: from 564 to 569.7 nm at a total density of absorbed pump energy of 800 J cm^{-3} (Fig. 2a), which can be related to the formation of photoproducts absorbing radiation in the short-wavelength region of the lasing spectrum. Studies must be continued to reveal the influence of 8MMA-POSS particles on the spectra and photostability of BODIPY derivatives. In this stage we can suggest that laser irradiation of a medium containing nanoparticles changes the fluctuations causing radiation scattering.

The lasing spectrum of the sample with the longest service life (BODIPY2 in PMMA, P_{90} = 3690 J cm^{-3}) undergoes the smallest shifts (1–0.7 nm), which is in agreement with the high photostability of this compound upon excitation at λ_p = 532 nm, and, correspondingly, weaker ability of causing spectral shifts in irradiated samples upon interaction with photoproducts.

4. Conclusions

Based on the results obtained, it was established that the spectral characteristics of BODIPY1 and BODIPY2 derivatives in a PMMA matrix are in qualitative agreement with the similar characteristics for solutions. Modification of matrices by 8MMA-POSS nanoparticles, which are capable of copolymerisation, as well as introduction of BODIPY derivatives into POSS-polymer films, changes only slightly the spectral characteristics but affects significantly the lasing efficiency and threshold.

The solid active medium based on BODIPY1 in a modified P(MMA + 8MMA-POSS) matrix was found to have the maximum efficiency: 90% instead of 70% for the unmodified matrix.

The highest lasing photostability at W_p = 3 MW cm^{-2} was obtained for the unmodified PMMA matrix coloured by BODIPY2 (P_{90} = 3690 J cm^{-3} or 7.4×10^9 J mol^{-1}, which corresponds to 10600 pump pulses absorbed by unit volume). It is undesirable to increase the pump intensity, because it leads to an increase in the lasing efficiency and intensity, which results in the fracture of PMMA matrices, both modified and unmodified.

The resource characteristics of BODIPY1 are only slightly improved in the modified matrix: from 720 to 762 J cm^{-3}; this increase is much smaller than that for BODIPY2 in unmodified PMMA. At the same time, proceeding from the number of lasing pulses at which EFF$_0$ decreases by 10%, the dependence is reverse: 4500 pulses for the pure PMMA matrix and 2400 pulses for the P(MMA + 8MMA-POSS) matrix, which is due to the difference in the volumes excited in these cases. The study must be continued to reveal the reason for the change in the excitation volumes.

The BODIPY derivatives analysed here are new active media. There are no data on their lasing characteristics in the literature, except for our previous studies on solutions of these compounds [6, 7]. Having compared the resource characteristics obtained by us for BODIPY1 and the data in the literature for the commercial BODIPY (PM567), which were reported in [9] for an unmodified PMMA matrix, we obtained the following estimates: P_{90} = 1.4×10^7 J mol^{-1} for BODIPY1 and $P_{90} \approx$ 1.5×10^7 J mol^{-1} for PM567. These values are in qualitative agreement with the photostability data obtained for ethanol solutions of compounds: P_{90} = 500 J cm^{-3} for BODIPY1 and P_{90} = 570 J cm^{-3} for PM567 [6]; this consistency indicates that the resource characteristics of BODIPY1 and PM567, which have similar structures, differ only slightly. At the same time, BODIPY2, which has a phenyl substituent in the *meso*-position of the BODIPY core, has a higher resource in both solutions and PMMA matrices under chosen excitation conditions.

The results of our study showed that, using the data on BODIPY derivatives, one can obtain efficient lasing in almost entire visible spectral range (470–620 nm) and outline ways for miniaturising laser media, which is important for practical applications.

Acknowledgements. This work was supported by the Russian Foundation for Basic Research (Grant No. 12-02-90008-Bel_a) and the Grant of the President of the Russian Federation for the State Support of Leading Scientific Schools (Grant No. NSh-512.2012.2).

References

1. Benstead M., Mehl G.H., Boyle R.W. *Tetrahedron*, **67**, 3573 (2011).
2. Loudet A., Burgess K. *Chem. Rev.*, **107**, 4891 (2007).

3. Shankarling G.S., Jarag K.L. *Resonance*, N 9, 804 (2010).
4. Costela A., Garcia-Morena I., Gomez C., Sastre R., Amat-Guerri F., Liras M., Lopez-Arbeloa F., Banuelos Prieto J., Lopez-Arbeloa I. *J. Phys. Chem. A*, **106**, 7736 (2002).
5. Costela A., Garcia-Moreno I., Sastre R. *Phys. Chem. Chem. Phys*., **5** (3), 4745 (2003).
6. Kuznetsova R.T., Aksenova Yu.V., Tel'minov E.N., Samsonova L.G., Mayer G.V., Kopylova T.N., Antina E.V., Yutanova S.L., Berezin M.B., Guseva G.B. *Opt. Spektrosk*., **112**, 785 (2012).
7. Kuznetsova R.T., Aksenova Yu.V., Orlovskaya O.O., Kopylova T.N., Tel'minov E.N., Mayer G.V., Antina E.V., Yutanova S.L., Berezin M.B., Guseva G.B., Antina L.A., Semeikin A.S. *Khim. Vys. Energ*., **46**, 464 (2012).
8. Cerdan L., Costela A., Garcia-Morena I., Garcia O., Sastre R. *Appl. Phys. B*, **97**, 73 (2009).
9. Costela A., Garcia-Moreno I., Barroso J., Sastre R. *Appl. Phys. B*, **70**, 367 (2000).
10. Jagtap K., Maity D., Ray A., Dasgupta K., Ghosh S. *Pramana*, **75**, 985 (2010).
11. Kopylova T.N., Anufrik S.S., Mayer G.V., Solodova T.A., Tel'minov E.N., Degtyarenko K.M., Samsonova L.G., Gadirov R.M., Nikonov S.Yu., Ponyavina E.N., Tarkovskii V.V., Sazonko G.G. *Izv. Vyssh. Uchebn. Zaved., Ser. Fiz*., **55** (10), 32 (2012).
12. Rubinov A.N., Anufrik S.S., Lyalikov A.M., Tarkovskii V.V., Sazonko G.G., Kopylova T.N., Solodova T.A., Degtyarenko K.M., Gadirov R.M., Tel'minov E.N., Ponyavina E.N. *Materialy mezhdunar. konf. 'Lazernaya fizika i primenenie lazerov'* (Proc. Int. Sci. Conf. 'Laser Physics and Laser Applications') (Grodno, 2012) Vol. 1, p. 176.
13. Liao Y., Meallet-Renault R., Audibert J.-F., Lemaistre J.-P., Clavier G., Retailleau P., Pansu R.B. *Phys. Chem. Chem. Phys.*, **15**, 3186 (2013).
14. Cerdan L., Costela A., Garcia-Moreno I., Garcia O., Sastre R. *Opt. Express*, **18** (10), 10247 (2010).
15. Pavlopoulos T., Boyer J.H., Shah M., Thangaroy K., Soong M.L. *Appl. Opt*., **29**, 3885 (1990).
16. Bañuelos J., Martín V., Gómez-Durán C.F.A., Córdoba I.J.A., Peña-Cabrera E., García-Moreno I., Costela Á., Pérez-Ojeda M.E., Arbeloa T., López-Arbeloa Í. *Chem. Eur. J*., **17**, 7261 (2011).
17. Perez-Ojeda M.E., Thivierge C., Martin V., Costela A., Burgess K., Carcia-Moreno I. *Opt. Mater. Express*, **1** (2), 243 (2011).
18. Costela A., Garcia Morena I., Cerdan L., Martin V., Garcia O., Sastre R. *Adv. Mater*., **21**, 4163 (2009).
19. Berezin M.B., Semeikin A.S., Antina E.V., Pashanova N.A., Lebedeva N.Sh., Bukushina G.B. *Zh. Obshch. Khim.*, **69**, 2040 (1999).
20. Berezin M.B., Semeikin A.S., Antina E.V., Guseva G.B., V'yugin A.I. *Zh. Obshch. Khim*., **82**, 1189 (2012).
21. Yutanova S.L., Berezin M.B., Semeikin A.S., Antina E.V., Guseva G.B., V'yugin A.I. *Zh. Obshch. Khim.*, **83**, 492 (2013).
22. Valiev R.R., Sinelnikov A.N., Aksenova Y.V., Kuznetsova R.T., Berezin M.B., Semeikin A.S., Cherepanov V.N. *Spectrochim. Acta A. Molecular and Biomolecular Spectroscopy*, **117**, 323 (2014).
23. Garcia O., Sastre R., Garcia-Moreno I., Martin V., Costela A. *J. Phys. Chem.*, **112**, 14710 (2008).
24. Kuznetsova R.T., Mayer G.V., Manekina Yu.A., Svetlichnyi V.A., Tel'minov E.N., Arabei S.M., Pavich T.A., Solov'ev K.N. *Opt. Spektrosk*., **102**, 234 (2007).